PHYSICAL REVIEW B VOLUME 40, NUMBER 18 15 DECEMBER 1989-II

Ab initio method for calculating response functions in transition metals

O. Gunnarsson
Max-Planck-Institut für Festkörperforschung, Heisenbergstrasse 1, D-7000 Stuttgart 80, West Germany

P. Gies and W. Hanke
Physikalisches Institut der Universität Würzburg, am Hubland, D-8700 Würzburg, West Germany

O. K. Andersen
Max-Planck-Institut für Festkörperforschung, Heisenbergstrasse 1, D-7000 Stuttgart 80, West Germany

(Received 14 August 1989)

We present a new approach for calculating charge- and spin-density response functions in transition metals from first principles, using tight-binding linear muffin-tin orbitals as basis functions. It is advantageous to use a partitioning in terms of small and large reciprocal-lattice vectors and to treat only the former exactly. We show that for the set of large reciprocal-lattice vectors, the dielectric matrix becomes separable, because only the plane-wave matrix elements between orbitals at the same lattice site contribute. Our method allows the evaluation of the electronic self-energy of transition metals within the *GW* approximation of Hedin [Phys. Rev. **139**, A796 (1965)].

I. INTRODUCTION

The variety of dynamical excitations in elementary transition metals[1,2] is mainly a consequence of the competing tendencies of the d electrons towards band formation on the one hand, and localization due to the Coulomb correlation on the other. Despite strong efforts during the last few decades,[3] and in striking contrast to the quantitative success of *ab initio* Hohenberg-Kohn density-functional methods using the Kohn-Sham local-density approximation (LDA) in describing ground-state properties,[4,5] electronic excitations are still far from being understood on a microscopic level. Previous many-body treatments on single- and two-particle excitations in transition metals have mostly relied on Hubbard-like models,[6–10] where the correlation energy U of the d electrons is treated as a parameter, which could be adjusted in such a way, that it fitted into the actual problem under study. Consequently, different values of U (e.g., for nickel) have been given in the literature.[6,11–14] First attempts to include interatomic correlation effects[15] used a Hubbard-like model as well.

Meanwhile, more reliable methods are available, which allow for the calculation of dynamical correlation effects from first principles, using Hedin's GW approximation.[16] In this theory, the electronic self-energy is expressed in terms of the single-particle Green's function (G) and the self-consistently screened Coulomb interaction (W), thus taking into account the strong correlation effects in the electronic system. However, due to the numerical complications of a GW-type calculation, this method has been applied, up to now, only to simple metals[17,18] and semiconductors.[19–21] A direct generalization of this work to transition metals seems to be impractible. The calculation of the screened interaction W, requires the calculation of the dielectric function ϵ and its inverse. In recent GW calculations,[17,18,20,21] ϵ was expressed as a matrix $\epsilon_{\mathbf{G},\mathbf{G}'}$, where $\mathbf{G}$ and $\mathbf{G}'$, are reciprocal-lattice vectors. While the number of important reciprocal-lattice vectors is manageable for simple metals and semiconductors in a pseudopotential treatment, this number becomes very large for transition metals, due to their compact d orbitals.

It seems promising to overcome this problem by changing to a local-orbital representation of the dielectric matrix, which is then separable in the reciprocal-lattice vectors.[22–24] In s-p–bonded semiconductors and insulators, by taking advantage of the directional properties of the hybridized s-p orbitals, the size of the dielectric matrix can be further reduced, and finally the computation becomes manageable.[19,24] In transition metals, however, this procedure is impractible, because the dielectric matrix remains very large, due to the large number of d orbitals and lattice sites involved. In earlier qualitative discussions,[22,25] only diagonal contributions from d electrons at the same site were considered, which is too crude an approximation in a quantitative analysis

Here we propose an efficient *ab initio* approach to calculate the dielectric-response properties of transition metals, using the Andersen linear muffin-tin orbitals (LMTO) method[26] in the tight-binding (TB) representation.[27] We show that a partitioning of the dielectric matrix can be attained in terms of two sets of small and large reciprocal-lattice vectors $\mathbf{G}$. Whereas the first set of $\mathbf{G}$ vectors (smaller than a certain limiting value, $|\mathbf{G}| < G_{\max}$) must be treated exactly, only the contributions from orbitals situated at the same crystal lattice site have to be retained in the second set of $\mathbf{G}$ vectors ($|\mathbf{G}| > G_{\max}$). One "subblock" of the dielectric matrix thus becomes separable, and the solution of the response equations becomes feasible.

The remainder of this paper is organized as follows: First, we explain how the dielectric matrix can be set up and inverted, using the partitioning approach. In the second part it is shown that this ansatz is justified in a standard transition metal (nickel) by computing the two-center integrals between TB LMTO's and plane waves, characterized by certain (small and large) wave vectors. Finally, we give a short summary and conclusions.

II. DIELECTRIC FUNCTION

We want to describe the electronic self-energy of a crystalline solid within the *GW* approximation.[16] This requires knowledge of the quasiparticle Green's function and the inverse of the dielectric function in the Bohm-Pines random-phase approximation (RPA). The RPA dielectric function is expressed in terms of the bare electronic polarizability function $p^0(\mathbf{q},\omega)$ and the unscreened Coulomb interaction $v(\mathbf{q})$ as

$$\epsilon(\mathbf{q},\omega)=1+p^0(\mathbf{q},\omega)v(\mathbf{q}) \ , \tag{1}$$

where $\mathbf{q}$ is the momentum in the first Brillouin zone and ω the frequency. Moreover, ϵ, 1, p^0, and v are matrices in the reciprocal-lattice ($\mathbf{G}$) representation whose elements are, respectively, $\epsilon_{\mathbf{G},\mathbf{G}'}(\mathbf{q},\omega)$, $\delta_{\mathbf{G},\mathbf{G}'}$, $p^0_{\mathbf{G},\mathbf{G}'}(\mathbf{q},\omega)$, and

$$v_{\mathbf{G},\mathbf{G}'}(\mathbf{q})\equiv 4\pi|\mathbf{q}+\mathbf{G}|^{-2}\delta_{\mathbf{G},\mathbf{G}'} \ . \tag{2}$$

where $\delta_{\mathbf{G},\mathbf{G}'}$ is the Kronecker symbol.

The matrix v is diagonal and p^0 is Hermitian. The problem is to solve the infinite matrix equation: $\epsilon^{-1}(1+p^0v)=1$.

The bare electronic polarizability can be expressed through the single-particle energies $E_{j\mathbf{k}\sigma}$ and wave functions $\Psi_{j\mathbf{k}\sigma}(\mathbf{r})\equiv|j\mathbf{k}\sigma\rangle$, j being the band index, $\mathbf{k}$ the Bloch vector, and σ the spin quantum number, as

$$p^0_{\mathbf{G},\mathbf{G}'}(\mathbf{q},\omega)=\sum_{j,j',\mathbf{k},\sigma}\frac{f_{j',\mathbf{k}+\mathbf{q},\sigma}-f_{j\mathbf{k}\sigma}}{E_{j',\mathbf{k}+\mathbf{q},\sigma}-E_{j\mathbf{k}\sigma}-\omega-i0^+}\langle j\mathbf{k}\sigma|e^{-i(\mathbf{q}+\mathbf{G})\cdot\mathbf{r}}|j',\mathbf{k}+\mathbf{q},\sigma\rangle\langle j',\mathbf{k}+\mathbf{q},\sigma|e^{i(\mathbf{q}+\mathbf{G}')\cdot\mathbf{r}'}|j\mathbf{k}\sigma\rangle \ . \tag{3}$$

Here, $f_{j\mathbf{k}\sigma}$ is the Fermi occupation number for state $j,\mathbf{k},\sigma$. A similar expression holds for the spin-density response function.[28–30] We shall assume that the single-particle energies and wave functions can be taken as the LDA eigenvalues and wave functions. The latter may then be expanded in terms of TB LMTO's,[27] $\chi_{\mathbf{R}L}(\mathbf{r}-\mathbf{R})$, situated at the atomic sites $\mathbf{R}$ and with the collective angular-momentum index L ($\equiv\{l,m\}$):

$$\Psi_{j\mathbf{k}\sigma}(\mathbf{r})=N^{-1/2}\sum_{\mathbf{R},L}\chi_L(\mathbf{r}-\mathbf{R})e^{i\mathbf{k}\cdot\mathbf{R}}b_{L,j\mathbf{k}\sigma} \ . \tag{4}$$

For the sake of simplicity, we merely consider the case of one atom per cell and assume that we can use the same orbitals for both spins. The matrix elements in (3) may then be expressed as

$$\langle j',\mathbf{k}+\mathbf{q},\sigma|e^{i(\mathbf{q}+\mathbf{G})\cdot\mathbf{r}}|j\mathbf{k}\sigma\rangle = \sum_{L,L'} b^*_{L';j',\mathbf{k}+\mathbf{q}\sigma}b_{L,j\mathbf{k}\sigma}\sum_{\mathbf{R}} e^{i\mathbf{k}\cdot\mathbf{R}}\mathcal{T}_{L'L\mathbf{R},\mathbf{G}}(\mathbf{q}) \ , \tag{5}$$

where

$$\mathcal{T}_{L'L\mathbf{R},\mathbf{G}}(\mathbf{q})\equiv\int\chi^*_{L'}(\mathbf{r})e^{i(\mathbf{G}+\mathbf{q})\cdot\mathbf{r}}\chi_L(\mathbf{r}-\mathbf{R})d^3r \tag{6}$$

is the Fourier transform of the product of two localized orbitals displaced by $\mathbf{R}$. The bare polarizability may, finally, be expressed by the matrix product

$$p^0(\mathbf{q},\omega)=\mathcal{T}^\dagger(\mathbf{q})P^0(\mathbf{q},\omega)\mathcal{T}(\mathbf{q}) \ , \tag{7}$$

where

$$P^0_{L_1L_2\mathbf{R}_2,L_3L_4\mathbf{R}_4}(\mathbf{q},\omega)=\sum_{j,j',\mathbf{k},\sigma}\frac{f_{j',\mathbf{k}+\mathbf{q},\sigma}-f_{j\mathbf{k}\sigma}}{E_{j'\mathbf{k}+\mathbf{q},\sigma}-E_{j\mathbf{k}\sigma}-\omega-i0^+}b_{L_1;j',\mathbf{k}+\mathbf{q},\sigma}b^*_{L_2,j\mathbf{k}\sigma}e^{i\mathbf{k}\cdot(\mathbf{R}_4-\mathbf{R}_2)}b^*_{L_3;j',\mathbf{k}+\mathbf{q},\sigma}b_{L_4,j\mathbf{k}\sigma} \tag{8}$$

is the bare polarizability in the representation of localized orbitals. In the matrix equations (1) and (7), and in the following, we use the convention that quantities expressed by lower-case letters are matrices in the reciprocal-lattice representation, quantities expressed by capital letters are matrices in the localized-orbital representation, and quantities expressed by script letters are (nonquadratic) matrices in the mixed representation.

The LMTO expansion (4) requires a finite number N_L of L values. For a transition metal, the five *nd* bands, the $(n+1)s$ band, and the three $(n+1)p$ bands are well described by a LMTO set having only one radial function per l value, i.e., by a minimal basis set, provided that the energies $E_{\nu l}$, about which the linear expansion of the radial functions are performed, are well chosen.[26] To describe the important unoccupied states, f orbitals ($l=3$) may also be needed. Hence, we expect reasonable accuracy for ϵ^{-1} with $N_L=9$ or $N_L=16$. Better accuracy may be obtained by including LMTO's with more radial functions. For TB LMTO's the product of two orbitals is non-negligible only for a relatively small number $N_R \approx 15$ of nearest- and (possibly) second-nearest-neighbor orbitals, and this holds not only for d LMTO's but for all TB LMTO's.[27] As a consequence, the number of rows in the matrix $\mathcal{T}$ is finite and equals $N_R(N_L)^2 \sim 10^3$. This is also the dimension of the square matrix P^0.

By virtue of (7), one obtains a matrix equation,

$$\epsilon^{-1}(1+\mathcal{T}^\dagger P^0 \mathcal{T} v)=1 \ , \tag{9}$$

which is separable:[22,23] Right multiplication by $\mathcal{T}^\dagger$ and definition of the finite-sized Hermitian matrix,

$$V(\mathbf{q}) \equiv \mathcal{T}(\mathbf{q}) v(\mathbf{q}) \mathcal{T}^\dagger(\mathbf{q}) \ , \tag{10}$$

which is the bare interaction in the localized-orbital representation, yields

$$\epsilon^{-1}\mathcal{T}^\dagger = \mathcal{T}^\dagger(1+P^0V)^{-1} \ . \tag{11}$$

When this is inserted back into (9), the result

$$\begin{aligned}\epsilon^{-1} &= 1-\mathcal{T}^\dagger(1+P^0V)^{-1}P^0\mathcal{T}v \\ &= 1-\mathcal{T}^\dagger[(P^0)^{-1}+V]^{-1}\mathcal{T}v\end{aligned} \tag{12}$$

is obtained. This shows that the infinite dielectric matrix may be inverted through inversion of the finite-sized matrix $1+P^0(\mathbf{q},\omega)V(\mathbf{q})$, or through inversion of the Hermitian matrices $P^0(\mathbf{q},\omega)$ and $[P^0(\mathbf{q},\omega)]^{-1}+V(\mathbf{q})$. For sp^3-bonded semiconductors, $N_L \approx 4$, and the directional character of the hybridized orbitals can be used to reduce the number of overlaps, N_R, so that the size $N_R(N_L)^2$ of the matrices becomes manageable.[24] For a transition metal, however, the matrix size cannot be reduced below $\approx 10^3$ and, since the inversions must be made for many values of $\mathbf{q}$ and ω, the calculation of P^0 and its inversion according to (12) is not practical for present-day computers.

Before explaining our modification to this scheme, we introduce a symmetrized dielectrix matrix[31,32] through

$$\tilde{\epsilon} \equiv v^{1/2}\epsilon v^{-1/2} = 1+v^{1/2}p^0 v^{1/2} = 1+\tilde{\mathcal{T}}^\dagger P^0 \tilde{\mathcal{T}} \ , \tag{13}$$

where we have defined

$$\tilde{\mathcal{T}} \equiv \mathcal{T} v^{1/2} \ , \tag{14}$$

with matrix elements $\mathcal{T}_{L'L\mathbf{R},\mathbf{G}}(\mathbf{q})(4\pi)^{1/2}|\mathbf{q}+\mathbf{G}|^{-1}$. The symmetrized dielectric matrix is thus expressed in terms of just two matrices, $P^0(\mathbf{q},\omega)$ and $\tilde{\mathcal{T}}(\mathbf{q})$. Left multiplication of (12) by $v^{1/2}$ and right multiplication by $v^{-1/2}$ now yields

$$\tilde{\epsilon}^{-1} = 1-\tilde{\mathcal{T}}^\dagger[(P^0)^{-1}+V]^{-1}\tilde{\mathcal{T}} \ . \tag{15}$$

where V may be expressed by

$$V = \tilde{\mathcal{T}}\tilde{\mathcal{T}}^\dagger \ . \tag{16}$$

To obtain a practical scheme for transition metals, we note that the product of two TB LMTO's centered at the same site has a different real-space behavior than the product of two orbitals centered at neighboring sites: The product of two orbitals on the same site is large and peaks at the atom, where it exhibits rapid variations. On the other hand, the product of two orbitals on neighboring sites is relatively small and peaks between the atoms, so that the rapid atomic variations are strongly damped. It therefore seems plausible that the Fourier components $\mathcal{T}_{L'L(\mathbf{R}\neq 0),\mathbf{G}}(\mathbf{q})$ of the neighbor-site overlaps can be neglected when $|\mathbf{G}|$ exceeds some reasonably low limit $G_{\max}$. We shall now label the subset of on-site local-orbital indices by "o", i.e., $(L'L\mathbf{R})_o \equiv (L',L,\mathbf{R}=\mathbf{0})$, and the subset of neighbor-site indices "n", i.e., $(L'L\mathbf{R})_n \equiv (L',L,\mathbf{R}\neq\mathbf{0})$. Whereas the number of local-orbital indices N_o+N_n is $(N_L)^2 N_R \approx 10^3$, the number of on-site indices N_o is only $(N_L)^2 \approx 10^2$. We shall, furthermore, label the subset of small $\mathbf{G}$ vectors "1," i.e., $|\mathbf{G}_1| \le G_{\max}$, and the subset of large $\mathbf{G}$ vectors "2," i.e., $|\mathbf{G}_2| > G_{\max}$. We expect that the number N_1 of small $\mathbf{G}$ vectors is of order 100. With $\tilde{\mathcal{T}}$ in block form we thus define

$$\tilde{\mathcal{T}} \equiv \begin{bmatrix} \tilde{\mathcal{T}}_{o1} & \tilde{\mathcal{T}}_{o2} \\ \tilde{\mathcal{T}}_{n1} & \tilde{\mathcal{T}}_{n2} \end{bmatrix} = \begin{bmatrix} \tilde{\mathcal{T}}_{o1} & \tilde{\mathcal{T}}_{o2} \\ \tilde{\mathcal{T}}_{n1} & 0 \end{bmatrix} \tag{17}$$

and hope that $G_{\max}$ can be chosen so small that the partition scheme to be described in the following will be practical.

Löwdin partitioning of the (symmetrized) dielectric matrix in the block form,

$$\tilde{\epsilon} = \begin{bmatrix} \tilde{\epsilon}_{11} & \tilde{\epsilon}_{12} \\ \tilde{\epsilon}_{21} & \tilde{\epsilon}_{22} \end{bmatrix} \ , \tag{18}$$

yields

$$(\tilde{\epsilon}^{-1})_{11} = [\tilde{\epsilon}_{11}-\tilde{\epsilon}_{12}(\tilde{\epsilon}_{22})^{-1}\tilde{\epsilon}_{21}]^{-1} \ . \tag{19}$$

Here, $(\tilde{\epsilon}^{-1})_{11}$ is the lower block of $\tilde{\epsilon}^{-1}$, whereas $(\tilde{\epsilon}_{22})^{-1}$ is the inverse of the higher block of $\tilde{\epsilon}$. The other blocks of $\tilde{\epsilon}^{-1}$ are given by

$$(\tilde{\epsilon}^{-1})_{21} = -(\tilde{\epsilon}_{22})^{-1}\tilde{\epsilon}_{21}(\tilde{\epsilon}^{-1})_{11} \tag{20}$$

and

$$(\tilde{\epsilon}^{-1})_{22} = (\tilde{\epsilon}_{22})^{-1}-(\tilde{\epsilon}^{-1})_{21}\tilde{\epsilon}_{12}(\tilde{\epsilon}_{22})^{-1} \ . \tag{21}$$

Now, the first problem is to invert ϵ_{22}. This matrix is given by the (2,2) block of (1) and, since v is diagonal, only the (2,2) blocks of p^0 and v are involved. The former is given by (7) as

$$p^0_{22} = (\tilde{\mathcal{T}}^\dagger)_{2o} P^0_{oo} \mathcal{T}_{o2} \ , \tag{22}$$

which, due to (17), only involves the on-site block of P^0. The inversion of ϵ_{22} is done by separation, as was described in Eqs. (9)–(16) with the difference that the indices $\mathbf{G}$ are now restricted to subset 2. This means that in (10) or (16) the internal summations only run over subset 2 and, using again (17), we see that the $V(\mathbf{q})$ involved vanishes outside the on-site block. It is given by

$$\hat{V}_{oo} = \mathcal{T}_{o2} v_{22} (\tilde{\mathcal{T}}^\dagger)_{2o} = \tilde{\mathcal{T}}_{o2}(\tilde{\mathcal{T}}^\dagger)_{2o} \ . \tag{23}$$

The result analogous to (15) is then

$$(\tilde{\epsilon}_{22})^{-1} = 1_{22}-(\tilde{\mathcal{T}}^\dagger)_{2o}[(P^0_{oo})^{-1}+\hat{V}_{oo}]^{-1}\tilde{\mathcal{T}}_{o2} \ . \tag{24}$$

This shows that $(\tilde{\epsilon}_{22})^{-1}$ may be obtained by inversion of only on-site block matrices with dimension $N_o \approx 10^2$. For use in (19)–(21) we furthermore need

$$\tilde{\epsilon}_{21} = (\tilde{\mathcal{T}}^{\dagger})_{2o}\mathcal{B}_{o1} , \tag{25}$$

as found from (12), making use of the fact that $(\tilde{\mathcal{T}}^{\dagger})_{2n} \equiv 0$. Here, $\mathcal{B}_{o1}$ is the lower block, of dimension $N_o \times N_1 \approx 10^2 \times 10^2$, of the bare polarizability in the mixed representation:

$$\mathcal{B}_{L'L0,\mathbf{G}_1}(\mathbf{q},\omega) \equiv \sum_{j,j',\mathbf{k},\sigma} b_{L';j',\mathbf{k}+\mathbf{q},\sigma} b^*_{L,j\mathbf{k}\sigma} \frac{f_{j',\mathbf{k}+\mathbf{q},\sigma} - f_{j\mathbf{k}\sigma}}{E_{j',\mathbf{k}+\mathbf{q},\sigma} - E_{j\mathbf{k}\sigma} - \omega - i0^+} \langle j',\mathbf{k}+\mathbf{q},\sigma | e^{i(\mathbf{q}+\mathbf{G}_1)\cdot\mathbf{r}} | j\mathbf{k}\sigma \rangle (4\pi)^{1/2} |\mathbf{q}+\mathbf{G}_1|^{-1} . \tag{26}$$

Combining (24) and (25), we then obtain

$$(\tilde{\epsilon}_{22})^{-1}\tilde{\epsilon}_{21} = (\tilde{\mathcal{T}}^{\dagger})_{2o}[1_{oo} + P^0_{oo}\hat{V}_{oo}]^{-1}\mathcal{B}_{o1} \tag{27}$$

which only requires operations with on-site blocks. For $(\tilde{\epsilon}^{-1})_{11}$ our final result is

$$(\tilde{\epsilon}^{-1})_{11} = \{\tilde{\epsilon}_{11} - (\mathcal{B}^{\dagger})_{1o}[(\hat{V}_{oo})^{-1} + P^0_{oo}]^{-1}\mathcal{B}_{o1}\}^{-1} , \tag{28}$$

which, in addition, requires the construction of $\tilde{\epsilon}_{11}$ from (3) and (12) and the subsequent inversion of a matrix of dimension $N_1 \times N_1$. The construction from (20) and (21) of the remaining blocks of ϵ^{-1} is straightforward if one uses (27); it merely requires summation over the reciprocal-lattice vectors of set 1.

In conclusion, our scheme for inverting the dielectric matrix, first of all, requires evaluation of the two-center integrals $\tilde{\mathcal{T}}(\mathbf{q})$ according to (6) and (14) for all Fourier components, and determination of the smallest possible $G_{\max}$ for which (17) is reasonably well satisfied. The inverse dielectric matrix is then evaluated using Löwdin partitioning: Eq. (28) yields the lower diagonal block, and (20) and (21) with (27) the remaining blocks. We first compute the on-site matrix elments $[\hat{V}(\mathbf{q})]_{oo}$ in the local-orbital representation of the high Fourier components of the Coulomb interaction according to (23) by summing to convergence over all $\mathbf{G}_2$ vectors. This matrix of size $N_o \times N_o$ ($\approx 10^2 \times 10^2$) is subsequently inverted. The on-site matrix elements $[P^0(\mathbf{q},\omega)]_{oo}$ of the bare polarizability in the local-orbital representation are calculated using (8), and then added to $\{[\hat{V}(\mathbf{q})]_{oo}\}^{-1}$ and inverted. The lower block $\mathcal{B}(\mathbf{q},\omega)_{o1}$ of the bare polarizability in the mixed representation is of size $N_o \times N_1 \approx 10^2 \times 10^2$ and is calculated according to (26). The lower block $\tilde{\epsilon}_{11}$ of the symmetrized dielectric matrix is, again, of size $\approx 10^2 \times 10^2$ and is calculated from (13) and (3). In (26) and (3) the number of matrix elements $\langle j',\mathbf{k}+\mathbf{q},\sigma | e^{i(\mathbf{q}+\mathbf{G}_1)\cdot\mathbf{r}} | j\mathbf{k}\sigma \rangle$, for each value of $\mathbf{k}$ and $\mathbf{q}$, equals the number of (j,j',σ) values, i,e., the number of interband transitions, times the number of $\mathbf{G}_1$ values. This yields about $10^2 \times 10^2$ matrix elements, and each of these are calculated from (5) which requires a summation over $(N_L)^2 N_R \approx 10^3$ terms. Finally, we need to invert the $\approx 10^2 \times 10^2$ matrix (28).

III. TWO-CENTER INTEGRALS

In this section we shall first explain how the two-center integrals $\mathcal{T}$ in (6) can be evaluated for TB LMTO's. We then calculate these integrals for the case of fcc Ni and show that the basic assumption of our method, namely that the high Fourier components of the product of two orbitals on different sites can be neglected, is justified. The calculations also show that a simplified evaluation of the integrals using the so-called atomic-spheres approximation may be sufficiently accurate in many cases.

A LMTO at site $\mathbf{R}$ may be evaluated in partial-wave components $\varphi_{L'}(\mathbf{r}-\mathbf{R}')$ about any site $\mathbf{R}'$ in the solid. Each expansion is valid inside the Wigner-Seitz (WS) cell surrounding that site and, if we define partial waves to vanish outside their respective cells, the LMTO may be expressed as[27]

$$\chi_L(\mathbf{r}-\mathbf{R}) = \varphi_L(\mathbf{r}-\mathbf{R}) + \sum_{\mathbf{R}',L'} \dot{\varphi}_{L'}(\mathbf{r}-\mathbf{R}') h_{\mathbf{R}'L',\mathbf{R}L} . \tag{29}$$

Here, the radial part φ_l is the solution of the radial Schrödinger equation at a chosen energy $E_{\nu l}$, and $\dot{\varphi}_l$ is the energy-derivative function appropriate for the TB representation. The expansion coefficients h form the effective two-center TB Hamiltonian.[27] With this cellular expansion the two-center integral (6) becomes

$$\begin{aligned}\mathcal{T}_{L'L\mathbf{R},\mathbf{G}}(\mathbf{q}) &= \int \chi^*_{L'}(\mathbf{r}) e^{i(\mathbf{G}+\mathbf{q})\cdot\mathbf{r}} \chi_L(\mathbf{r}-\mathbf{R}) d^3r \\ &= \langle \varphi_{L'} | e^{i(\mathbf{q}+\mathbf{G})\cdot\mathbf{r}} | \varphi_L \rangle \delta_{0,\mathbf{R}} + \sum_{L_1} (h_{0L',\mathbf{R}L_1} \langle \dot{\varphi}_{L_1} | e^{i(\mathbf{q}+\mathbf{G})\cdot\mathbf{r}} | \varphi_L \rangle e^{i\mathbf{q}\cdot\mathbf{R}} + \langle \varphi_{L'} | e^{i(\mathbf{q}+\mathbf{G})\cdot\mathbf{r}} | \dot{\varphi}_{L_1} \rangle h_{0L_1,\mathbf{R}L}) \\ &\quad + \sum_{\mathbf{R}_1} e^{i\mathbf{q}\cdot\mathbf{R}_1} \sum_{L_1,L_2} h_{0L',\mathbf{R}_1L_1} \langle \dot{\varphi}_{L_1} | e^{i(\mathbf{q}+\mathbf{G})\cdot\mathbf{r}} | \dot{\varphi}_{L_2} \rangle h_{\mathbf{R}_1L_2,\mathbf{R}L} .\end{aligned} \tag{30}$$

Here, all cellular integrals $\langle \cdots \rangle$ have been shifted to the cell at the origin, thus giving rise to the factors $e^{i\mathbf{q}\cdot\mathbf{R}}$. We follow the common practice of not performing the tedious cellular integrals, but instead first approximate the cells by spheres of the same volume [atomic-spheres approximation (ASA)] and then perform a so-called combined correction.[26,27] In the ASA we simply have

$$\langle \varphi_{L'}|e^{i\mathbf{K}\cdot\mathbf{r}}|\varphi_L\rangle = \sum_{l''} 4\pi i^{l''} Y^*_{l''(m'-m)}(\hat{\mathbf{K}}) C_{LL'L''} \int_0^w j_{l''}(Kr)\varphi_l(r)\varphi_{l'}(r) r^2\, dr \,, \tag{31}$$

in terms of the Gaunt coefficients $C_{LL'L''} \equiv \langle Y_{L'}|Y_{L''}|Y_L\rangle$ and radial integrals. The WS radius is w. An analogous expression holds for the other one-center integrals in (30).

Performing the integrals over space-filling WS spheres means that certain parts of space are double counted, and other parts are neglected. In addition, the summations over L_1 and L_2 in Eq. (30) are cut off at $l > 2$, although there are non-negligible contribution from higher angular-momentum values. To correct for these two deficiencies, we introduce the TM LMTO's $\chi^{\mathrm{ps}}_{\mathbf{R}L}$ for a flat potential and normalize these smooth pseudo-orbitals such that they match the nickel TB LMTO's at all the WS spheres in the solid.[26] Since both $\chi_{\mathbf{R}L}$ and $\chi^{\mathrm{ps}}_{\mathbf{R}L}$ are continuous and continuously differentiable with the same envelope function, they are very similar in the outer parts of the WS spheres. This is illustrated for the central sphere in Fig. 1, which shows the $4s$, $4p_y$, and $3d_{xy}$ orbitals along the direction [110] towards a nearest neighbor. For the s and p orbitals, the agreement is very good for $0.6 < r/w \le 1$, while for the d orbitals the agreement is limited to $0.9 < r/w \le 1$. Since for a fcc lattice the closest approach of one WS sphere to the center of another is $0.8w$, the real and the pseudo-orbitals agree almost throughout the overlap region. We then have

$$\begin{aligned} \mathcal{T}_{L'L\mathbf{R},\mathbf{G}}(\mathbf{q}) = \int \chi^*_{L'}(\mathbf{r}) e^{i(\mathbf{G}+\mathbf{q})\cdot\mathbf{r}} \chi_L(\mathbf{r}-\mathbf{R})\, d^3r \approx & \int \chi^{*\mathrm{ps}}_{L}(\mathbf{r}) e^{i(\mathbf{G}+\mathbf{q})\cdot\mathbf{r}} \chi^{\mathrm{ps}}_L(\mathbf{r}-\mathbf{R})\, d^3r \\ & - \int_{\mathrm{ASA}} \chi^{*\mathrm{ps}}_{L}(\mathbf{r}) e^{i(\mathbf{G}+\mathbf{q})\cdot\mathbf{r}} \chi^{\mathrm{ps}}_L(\mathbf{r}-\mathbf{R})\, d^3r \\ & + \int_{\mathrm{ASA}} \chi^*_{L'}(\mathbf{r}) e^{i(\mathbf{G}+\mathbf{q})\cdot\mathbf{r}} \chi_L(\mathbf{r}-\mathbf{R})\, d^3r \,. \end{aligned} \tag{32}$$

The last two integrals are performed according to (31) in the ASA, while the first integral is calculated without any shape approximation. This calculation is feasible, due to the slowly varying character of the pseudo-orbitals and their short range. In performing the first integral, we use a three-dimensional grid in real space, and we employ the three-dimensional equivalent of Filon's method[33] in order to take into account the oscillating behavior of the plane wave factor.

Results for the two-center integrals calculated with and without the ASA for fcc nickel are shown in Fig. 2 for $L = L'$, $\mathbf{q} = 0$, and different choices of $\mathbf{R}$ and $\mathbf{G}$, This

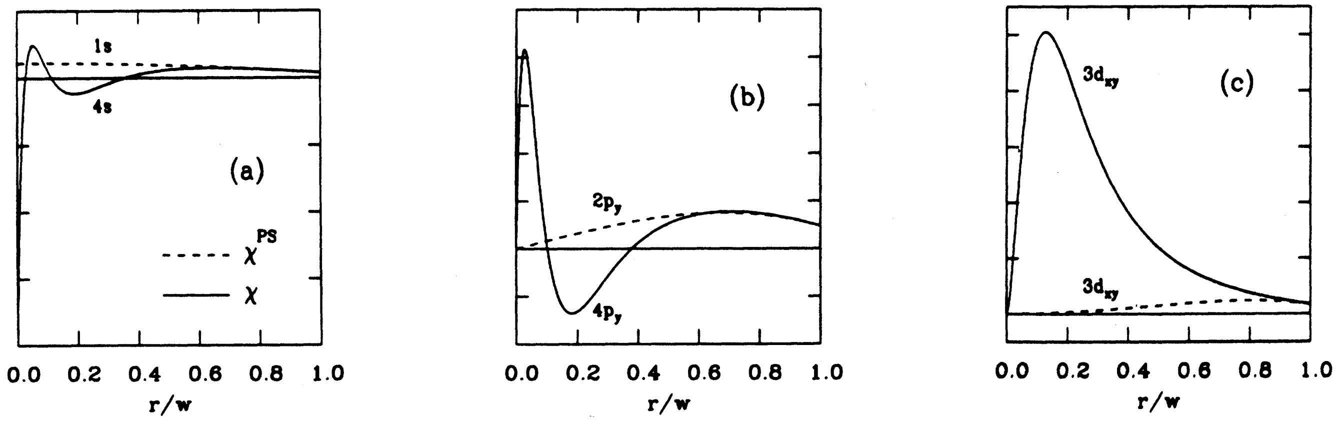

FIG. 1. (a) $4s$, (b) $4p_y$, and (c) $3d_{xy}$ TB orbitals for nickel (solid lines), as compared to the corresponding pseudo-orbitals (dashed lines), plotted in atomic units along the [110] direction for $0 \le r/w \le 1$ (with w the WS radius).

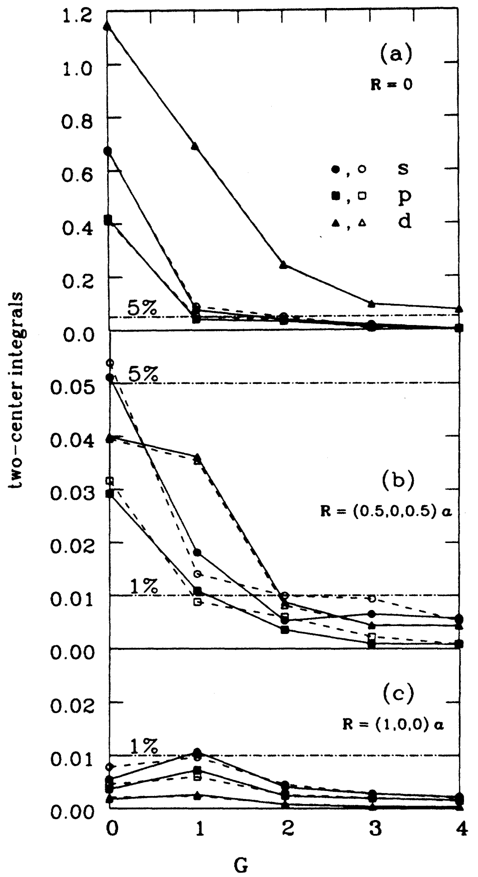

FIG. 2. Averaged, diagonal two-center integrals for nickel [cf. Eqs. (32) and (33)] for $l=0$ (s), $l=1$ (p), and $l=2$ (d), plotted vs $\mathbf{G}\equiv(G,G,G)$ for $G=0$, 1, 2, 3, and 4 in units of $2\pi/a$ and $q=0$. (a) On-site term, $\mathbf{R}=\mathbf{0}$, (b) nearest-neighbor term, $\mathbf{R}=(0.5,0,0.5)a$, and (c) next-nearest-neighbor term, $\mathbf{R}=(1,0,0)a$. The solid symbols show the results with pseudo-orbital corrections [cf. Eq. (32)] and the open symbols the ASA results. Note that in (b) and (c) the scale is enlarged. The straight and dashed lines are a guide to the eye. The horizontal lines show 1% and 5% of the maximum value of $\mathcal{T}$.

figure shows the averaged matrix elements

$$\left[(2l+1)^{-1}\sum_{m}|\mathcal{T}_{LL\mathbf{R},\mathbf{G}}(\mathbf{q})|^2\right]^{1/2} \tag{33}$$

for $l=0$, 1, and 2. The on-site ($\mathbf{R}=\mathbf{0}$) result [Fig. 2(a)] decays rather rapidly with G for the s and p orbitals, while for the d orbitals the decay is much slower. This is due to the relatively large weight of the nonpseudo part of the d orbitals, and it is the reason why transition metals are much more difficult to treat than s-p-bonded systems. In Fig. 2(b), results are shown for the two-center integrals, when the two orbitals are centered at nearest-neighbor atoms. These integrals are typically an order of magnitude smaller than the on-site integrals. This is due to the fast decay of the TB orbitals. Results are also shown, in Fig. 2(c), for orbitals centered on the second-nearest-neighbor sites. In view of Fig. 2, one can probably neglect all off-site matrix elements for reciprocal-lattice vectors larger than $(2,2,2)(2\pi/a)$. In set 1 there are then $N_1=59$ $\mathbf{G}$ vectors. The matrix elements in set 2 are then 1% or less of the maximum value. This assumption is further substantiated by the structure of the electronic polarizability matrix P^0 in the local-orbital representation, Eq. (8). If $\mathbf{R}_2\neq\mathbf{R}_4$, the oscillating factor $e^{i\mathbf{k}\cdot(\mathbf{R}_4-\mathbf{R}_2)}$ will strongly reduce the corresponding matrix element. If, on the other hand, $\mathbf{R}_2=\mathbf{R}_4$, the neglected term contains a factor $\mathcal{T}\mathcal{T}^\dagger$, which is of the order of $\leq 10^{-4}$.

The open symbols in Fig. 2 show results in the ASA. The relative errors are small for the on-site terms and larger for the off-site terms, while the opposite is true for the absolute errors. The largest error is about 1% of the maximum value of $\mathcal{T}$.

IV. CONCLUSIONS

In conclusion, we have presented a method for calculating and inverting the dielectric matrix for systems, where many reciprocal-lattice vectors $\mathbf{G}$ are needed. We partitioned the G's into two sets with N_1 ($|\mathbf{G}|\leq G_{\max}$) and N_2 ($|\mathbf{G}|>G_{\max}$) vectors, respectively, according to their magnitude. For the N_1 vectors in set 1, the dielectric matrix is calculated exactly, while for the vectors in set 2, the two-center integrals $\mathcal{T}_{L'L\mathbf{R},\mathbf{G}}(\mathbf{q})$ [Eq. (6)] are neglected unless $R=0$ (on-site terms). For nickel we find that this should be a rather good approximation, if $N_1\cong 100$. The approximation makes the dielectric matrix separable in G_2 and G_2'. If we assume that N_L (~ 9 or 16) orbitals per site are needed to describe the system, and that a given orbital has a non-negligible overlap with orbitals on N_R sites ($N_R\approx 12-18$ for a fcc lattice), the calculation of ϵ^{-1} involves the calculation of matrices of the dimension $\max[N_1,N_L^2]$, instead of N_1+N_2 or $N_\mathbf{R}N_L^2$, as in earlier approaches.

ACKNOWLEDGMENTS

One of us (P.G.) acknowledges financial support by the Deutsche Forschungsgemeinschaft (DFG) under Grant No. Ha-1537/1-1. We want to thank P. Blöchl and M. Schilfgaarde for providing parts of the computer code.

---

[1] D. E. Eastman, F. J. Himpsel, and J. A. Knapp, Phys. Rev. Lett. **44**, 95 (1980); W. Eberhardt and E. W. Plummer, Phys. Rev. B **21**, 3245 (1980); L. C. Davis, J. Appl. Phys. **59**, R25 (1986).

[2] W. Speier, R. Zeller, and J. C. Fuggle, Phys. Rev. B **32**, 3597 (1985); L. E. Klebanoff *et al.*, *ibid.* **36**, 7849 (1987).

[3] For a review, see P. Fulde, Y. Kakehashi, and G. Stollhoff, in *Topics in Current Physics,* Vol. 42 of *Metallic Magnetism,*

edited by H. Capellmann (Springer, Berlin, 1987), p. 159.

[4] V. L. Moruzzi, J. F. Janak, and A. R. Williams, *Calculated Electronic Properties of Metals* (Pergamon, New York, 1978).

[5] A. R. Mackintosh and O. K. Andersen, in *Electrons at the Fermi Surface,* edited by M. Springford (Cambridge University Press, Cambridge, 1980).

[6] G. Treglia, F. Ducastelle, and D. Spanjaard, J. Phys. (Paris) **41**, 281 (1980); **43**, 341 (1982).

[7] J. Kanamori, in *Electronic Correlation and Magnetism in Narrow-Band Systems,* edited by T. Moriya (Springer, Berlin, 1981), pp. 102 and 109.

[8] A. Liebsch, Phys. Rev. B **23**, 5203 (1981).

[9] L. Kleinman and K. Mednick, Phys. Rev. B **24**, 6880 (1981).

[10] A. M. Oles and G. Stollhoff, Phys. Rev. B **29**, 314 (1984).

[11] C. Herring, in *Magnetism,* edited by G. T. Rado and H. Shul (Academic, New York, 1966), Vol. IV, Chap. IX.

[12] B. N. Cox, M. A. Coulthard, and P. Lloyd, J. Phys. F **4**, 807 (1974).

[13] L. C. Davis and L. A. Feldkamp, J. Appl. Phys. **50**, 1944 (1979).

[14] T. Bandyopadhyay and D. D. Sarma, Phys. Rev. B **39**, 3517 (1989).

[15] T. Aiska, T. Kato, and E. Haga, Phys. Rev. B **28**, 1113 (1983).

[16] L. Hedin, Phys. Rev. **139**, A796 (1965); L. Hedin and S. Lundqvist, in *Solid State Physics,* edited by F. Seitz and D. Turnbull (Academic, New York, 1968), Vol. 23, p. 1.

[17] P. Horsch, W. von der Linden, and W.-D. Lukas, Solid State Commun. **62**, 359 (1987).

[18] J. E. Northrup, M. S. Hybertsen, and S. G. Louie, Phys. Rev. Lett. **59**, 819 (1987); Phys. Rev. B **39**, 8198 (1989).

[19] G. Strinati, H. J. Mattausch, and W. Hanke, Phys. Rev. B **25**, 2867 (1982).

[20] M. S. Hybertsen and S. G. Louie, Phys. Rev. Lett. **55**, 1418 (1985); Phys. Rev. B **34**, 5390 (1986).

[21] R. W. Godby, M. Schlüter, and L. J. Sham, Phys. Rev. Lett. **56**, 2415 (1986); Phys. Rev. B **35**, 4170 (1987); **37**, 10 159 (1988).

[22] L. J. Sham, Phys. Rev. B **6**, 3584 (1972).

[23] W. Hanke, Phys. Rev. B **8**, 4585 (1973).

[24] W. Hanke and L. J. Sham, Phys. Rev. Lett. **33**, 582 (1974); Phys. Rev. B **12**, 4501 (1975).

[25] E. Hayashi and M. Shimizu, J. Phys. Soc. Jpn. **26**, 1396 (1969); S. K. Sinha, Phys. Rev. **177**, 1256 (1969).

[26] O. K. Andersen, Phys. Rev. B **12**, 3060 (1975).

[27] O. K. Andersen and O. Jepsen, Phys. Rev. Lett. **53**, 2571 (1984); O. K. Andersen, Z. Pawlowska, and O. Jepsen, Phys. Rev. B **34**, 5253 (1986); P. Blöchl, Ph.D. thesis, University of Stuttgart, 1989.

[28] J. F. Cook, J. W. Lynn, and H. L. Davis, Phys. Rev. B **21**, 4118 (1980).

[29] J. Callaway, A. K. Chatterjee, S. P. Singhal, and A. Ziegler, Phys. Rev. B **28**, 3818 (1983).

[30] E. Stenzel, H. Winter, Z. Szotek, and W. M. Temmermman, Z. Phys. B **70**, 173 (1988).

[31] A. Baldereschi and E. Tosatti, Solid State Commun. **29**, 131 (1979).

[32] R. Car, E. Tosatti, S. Baroni, and S. Leelaprute, Phys. Rev. B **24**, 985 (1981).

[33] *Handbook of Mathematical Functions, 9th ed.,* edited by M. Abramowitz and I. A. Stegun (Dover, New York, 1972), p. 890.